

# The Incipience of Nucleate Boiling in Forced Convection Flow

E. J. DAVIS and G. H. ANDERSON

Imperial College, London, England

An analysis of the incipience of nucleate boiling is developed as a modification and extension of previous analyses. The results are compared with data for the subcooled boiling of water in forced convection flow. Apparent anomalies in the data for the onset of boiling in two-phase gas-liquid flow are shown to be a result of a limited size range of cavities on the heater surfaces. Measurements of the surface characteristics of a copper heating tube were made and compared with incipient boiling heat transfer data taken in that tube. The results predicted from the theoretical analysis are consistent with the experimental heat transfer data.

The applications of nucleate boiling have been widely discussed in the literature, and the number of papers on the subject is legion, as indicated by the literature survey of boiling by Leppert and Pitts (1). In a number of processes involving evaporation of a liquid, however, nucleate boiling may not be a desirable phenomenon (for example, in thin film evaporators for saline water purification). Here it is important to be able to predict the onset of nucleate boiling.

In heat transfer systems involving two-phase gas-liquid flow it has been observed that nucleate boiling is suppressed at higher vapor fractions and/or higher mass velocities (2 to 6). This suppression of nucleate boiling is essentially the same problem as the initiation of nucleate boiling, the distinction being the direction from which the critical temperature difference required to sustain nucleation and bubble growth is approached. Therefore information on the conditions required for the onset of nucleate boiling would be useful in the design of two-phase flow heat transfer equipment.

Dengler (2), in an investigation of heat transfer to water in a vertical tube evaporator, attempted to correlate the minimum temperature difference required to initiate nucleate boiling with the average velocity of the liquid phase, but his correlation was found to be not generally valid (3). Hsu (7) developed a theory for the onset of nucleate boiling by using a model of Hsu and Graham (8) which related the size range of active nucleation sites on a heating surface to the superheat required to initiate nucleate boiling in the liquid. Application of the Hsu theory requires knowledge of the limiting thermal layer thickness within which a bubble nucleus can develop, but it is not yet possible to predict this boundary-layer thickness from theory for the pool boiling situation considered by Hsu.

Han and Griffith (9) proposed an analysis similar to Hsu's, and Bergles and Rohsenow (10, 11) adapted the Han and Griffith analysis to develop a criterion for the onset of nucleate boiling for a system with a wide range of cavity sizes. Assuming a linear temperature profile in the vicinity of a hemispherical bubble nucleus and using an equilibrium theory to describe the superheat needed for equilibrium of the bubble, they developed a graphical technique for predicting the onset of significant nucleate boiling that was in good agreement with their data for water in forced convection flow in stainless steel and nickel tubes. From their graphical calculations they established the following design equation for the heat flux required to initiate nucleate boiling in water:

$$q_{wi} = 15.60 p^{1.156} (T_w - T_s)^{2.30/p^{0.0234}} \quad (1)$$

As Bergles and Rohsenow pointed out, the method is restricted to systems that have cavity sizes in a wide range, which should apply to many commercial surfaces, but they did not attempt to prescribe the range required.

Sato and Matsumura (12) developed an analytical treatment equivalent to that of Bergles and Rohsenow, and they compared their analysis with their measurements of the incipience of nucleate boiling of water at atmospheric pressure flowing in a rectangular duct with a stainless steel heat transfer surface. They proposed the following equation for the heat flux required to initiate nucleate boiling:

$$q_{wi} = \frac{k_L \lambda \rho_v}{8 \sigma T_s} (T_w - T_s)^2 \quad (2)$$

Kenning (13), incorporating the results of his studies of flow around single bubbles at a wall and the assumptions involved in the Bergles and Rohsenow theory, developed an empirical correlation for the wall superheat ( $T_w - T_s$ ) required to initiate nucleate boiling. His anal-

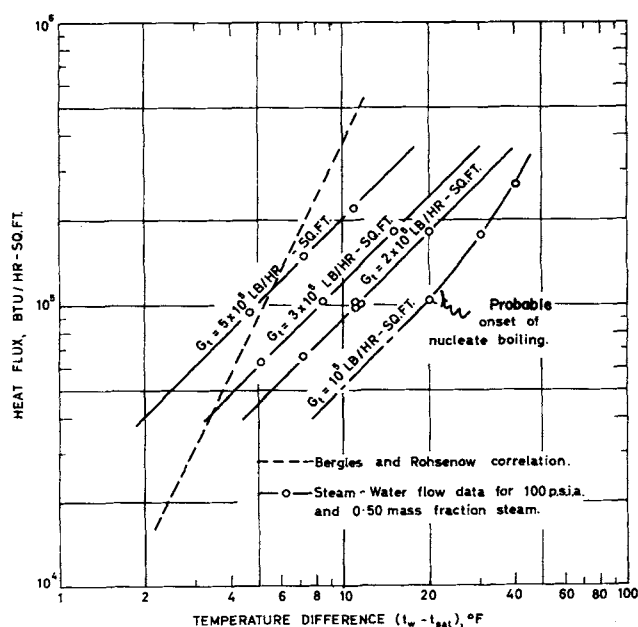


Fig. 1. A comparison of previous analyses with two-phase flow heat transfer data.

ysis predicts wall superheats that are considerably lower than those predicted by the former analysis.

If a smooth surface is involved Equations (1) and (2) can be in great error at moderate heat fluxes, for the onset of nucleate boiling can be restricted by a lack of larger cavities. Gouse and Coumou (14) discussed the suppression of nucleate boiling in their study of heat transfer to Freon-113 in a Pyrex tube, which they claimed, had cavity sizes of 40  $\mu$  in. or less. A similar situation can occur if metallic surfaces are involved.

Figure 1 is an example of the error that can occur with the use of the Bergles and Rohsenow or Sato and Matsumura results. The figure compares Equation (1) with steam-water two-phase annular flow heat transfer data of Davis (15) taken in a 302 stainless steel duct which had a very smooth surface. The lines of unit slope indicate that forced convection non-nucleate boiling predominated at temperatures differences considerably greater than the incipient boiling temperature differences predicted from Equation (1). For the conditions given in Figure 1 and at total mass velocities less than 10<sup>5</sup> lb./ (hr.) (sq. ft.) nucleate boiling was found to occur. The heat fluxes in Figure 1 are lower than those studied by Bergles and Rohsenow, but the results indicate that no cavities were activated except at the lower mass flow rates and at temperature differences greater than 20°F.

Data taken by Mantzouranis (16) with water boiling in a vertical tube evaporator show similar disagreement with the Bergles and Rohsenow analysis; these data will be discussed in greater detail below.

It will be shown that the inconsistencies in data reported in the heat transfer literature on the incipience of nucleate boiling and the disagreement between theoretical analyses and some experimental data are due to characteristics of the heat transfer surface. By modifying the Bergles and Rohsenow analysis, analytical solutions for the wall superheat required to initiate nucleate boiling and for the critical cavity size (the size of the first cavities to become active as the wall temperature is increased) can be obtained.

## ANALYSIS

The following assumptions are involved in the mathematical model:

1. The bubble nucleus, which develops at a surface cavity, has the shape of a truncated sphere.
2. Equilibrium theory can be used to predict the superheat required to satisfy a force balance on the bubble.
3. A bubble nucleus will grow if the temperature of the fluid at a distance from the wall equal to the bubble height is greater than the superheat required for bubble equilibrium.
4. The bubble nucleus does not alter the temperature profile in the fluid surrounding it.

Figure 2 shows three possible bubble nucleus shapes. Bergles and Rohsenow assumed a hemispherical bubble, case II, arguing that once a bubble has passed this condition of minimum radius it will continue to grow. In a

nonuniform temperature field it is possible for the bubble nucleus to assume some other equilibrium state, say case I or case III in Figure 2. Whether a variation of surface tension with temperature results in a stable nonspherical bubble, case I, or whether equilibrium is actually a steady state condition with heat and mass transfer into the base of the bubble offset by loss at the top of it, is open to speculation. For the purposes of this discussion we shall assume a truncated spherical bubble, case III, which reduces to the hemispherical bubble when the bubble contact angle is 90 deg. It is possible that the nucleus will not grow much beyond the hemispherical shape even if the superheat is sufficient, for shear forces acting on the bubble can sweep it from the wall. The hemispherical bubble will have the greater stability.

Zuber (17) pointed out that the equilibrium theory used by Hsu does not rigorously apply to a bubble in a nonisothermal field, but it will be used here as a reasonable first approximation.

Assumption 3 is the criterion suggested by Bergles and Rohsenow for the incipience of nucleate boiling. Both Sato and Matsumura and Kenning have suggested alternatives to this assumption that lead to lower predicted values of the wall superheat required to initiate nucleate boiling, arguing that a more suitable isothermal streamline is one nearer the wall since the bubble disturbs the flow. Because the choice of the isothermal streamline is somewhat arbitrary, the limiting case used by Bergles and Rohsenow is employed here.

Since cavities in only a narrow size range are involved at the onset of nucleate boiling, it is expected that the population density of bubbles on the surface just prior to the onset of nucleate boiling will be so low that they will not greatly affect the temperature profile in the fluid. Because the bubble nuclei are very small they are within the laminar sublayer where heat transport occurs by conduction through the liquid.

## THE SUPERHEAT EQUATION

The equation that describes the superheat required for a stable bubble is established by combining the Gibbs equation for the pressure difference across a curved surface, the Clausius-Clapeyron equation, and the ideal gas law as follows: By assuming that  $\rho_L \gg \rho_v$  and that the vapor density can be determined from the ideal gas law, that is,  $\rho_v = p/RT$ , the Clausius-Clapeyron equation becomes

$$\frac{dp}{dT} = \frac{\lambda p}{RT^2} \quad (3)$$

Integrating this expression between  $p_s, T_s$  and  $p_b, T_b$ , and substituting the Gibbs equation

$$p_b - p_s = 2\sigma/r_b \quad (4)$$

in the integrated equation give the superheat equation:

$$T_b - T_s = \frac{RT_b T_s}{\lambda} \ln (1 + 2\sigma/r_b p_s) \quad (5)$$

For low superheats or at higher pressures Equation (5) reduces to the superheat equation used in previous analyses (7, 12, 13):

$$T_b - T_s = \frac{2\sigma T_s}{\lambda \rho_v} \quad (6)$$

but Equation (5) is generally more valid.

It is convenient to write the superheat equations in terms of the bubble height or distance from the wall to the top of the bubble,  $y_b$ . The relationships between the bubble height, the bubble radius  $r_b$ , and the cavity radius  $r_c$  are

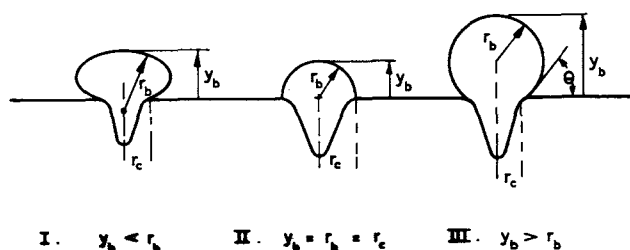


Fig. 2. Possible bubble models.

$$y_b = r_b (1 + \cos \theta) = C_1 r_b \quad (7)$$

and

$$r_c = r_b \sin \theta = C_2 r_b \quad (8)$$

where  $\theta$  is the contact angle indicated in Figure 2. Griffith and Wallis (18) measured bubble contact angles for water on clean surfaces, and they reported typical contact angles for contaminated metal surfaces which ranged from about 30 to 90 deg. These results indicate that engineering surfaces are usually partially wetted by water and organic liquids.

By using Equation (7) the superheat equation can be rewritten as

$$T_b - T_s = \frac{RT_b T_s}{\lambda} \ln (1 + 2C_1 \sigma / y_b p_s) \quad (9)$$

Since it is assumed that nucleate boiling will occur if the temperature at  $y_b$  is greater than  $T_b$  given by the superheat equation, it is necessary to write an expression for the temperature profile in the liquid to establish the criterion analytically.

### THE TEMPERATURE PROFILE

By assuming that the fraction of the heater surface covered by bubble nuclei is small, that the bubble nuclei develop well within the laminar sublayer, and that the thermal conductivity of the liquid is constant, a linear temperature profile can be assumed for the liquid:

$$T = T_w - q_w y / k_L \quad (10)$$

### THE CRITERION FOR THE ONSET OF NUCLEATE BOILING

The incipience of nucleate boiling depends on the existence of active cavities as well as a temperature profile that can satisfy the superheat requirement. If a sufficiently wide range of cavity sizes is involved the first cavities to become active will be those corresponding to the point of tangency of the superheat curve and the temperature profile curve as indicated by curve A in Figure 3. The temperature profiles in Figure 3 are shown as curved purely for illustrative purposes, and the analytical treat-

ment is confined to the linear portion of the curves. In the figure  $y'$  is the distance from the wall that equals the equilibrium bubble nucleus height. The critical cavity radius  $r_c'$  that corresponds to  $y'$  is, from Equations (7) and (8)

$$r_c' = \frac{C_2}{C_1} y' \quad (11)$$

Bubble growth may occur at a somewhat lower temperature than that indicated because the lower part of the bubble nucleus is in contact with fluid hotter than  $T'$ , but the assumed criterion does establish an upper limit to the wall superheat ( $T_w - T_s$ ) required to initiate nucleate boiling when a wide range of cavity sizes exists.

If no cavities of the size  $r_c'$  exist, nucleate boiling will not occur until the wall temperature is increased to the point that existing cavities are activated by supplying the local superheat required for bubble growth. Illustratively this condition is the intersection of the superheat and temperature profile curves at points that correspond to existing potentially active cavities, for example, curve B in Figure 3.

The curves represented by Equations (9) and (10) have slopes

$$\frac{dT}{dy} = -q_w / k_L \quad (12)$$

and

$$\frac{dT_b}{dy_b} = - \frac{2C_1 R T_s^2}{p_s y_b^2 (1 + \xi)} \left[ 1 - \frac{RT_s}{\lambda} \ln(1 + \xi) \right]^{-2} \quad (13)$$

where

$$\xi = 2\sigma C_1 / p_s y_b$$

Except for conditions involving very high wall superheats, Equation (13) can be simplified with slight loss in accuracy, for in most cases

$$1 \gg \frac{RT_s}{\lambda} \ln(1 + \xi)$$

Hence Equation (13) simplifies to

$$\frac{dT_b}{dy_b} = - \frac{2C_1 S}{y_b^2 (1 + \xi)} \quad (14)$$

where

$$S = \sigma T_s / \lambda p_v$$

By equating the slopes of the superheat equation and the temperature profile and by solving for the critical distance  $y'$  one obtains

$$y' = \frac{C_1 \sigma}{p_L} + \sqrt{\left( \frac{C_1 \sigma}{p_L} \right)^2 + \frac{2C_1 k_L S}{q_w}} \quad (15)$$

Substitution of  $y'$  from Equation (15) into Equation (9) and elimination of  $T'$  give the following expression for the wall superheat required to initiate nucleate boiling, provided that cavities of the size corresponding to  $y'$  exist:

$$T_w - T_s = \frac{\frac{RT_s^2}{\lambda} \ln(1 + \xi')}{1 - \frac{RT_s}{\lambda} \ln(1 + \xi')} + \frac{q_w y'}{k_L} \quad (16)$$

where  $\xi' = 2\sigma C_1 / p_s y'$ , and  $y'$  is given by Equation (15).

For systems at higher pressures or for low surface tension considerable simplification is possible. Under these conditions Equation (13) approximates to

$$\frac{dT_b}{dy_b} = \frac{-2C_1 S}{y_b^2} \quad (17)$$

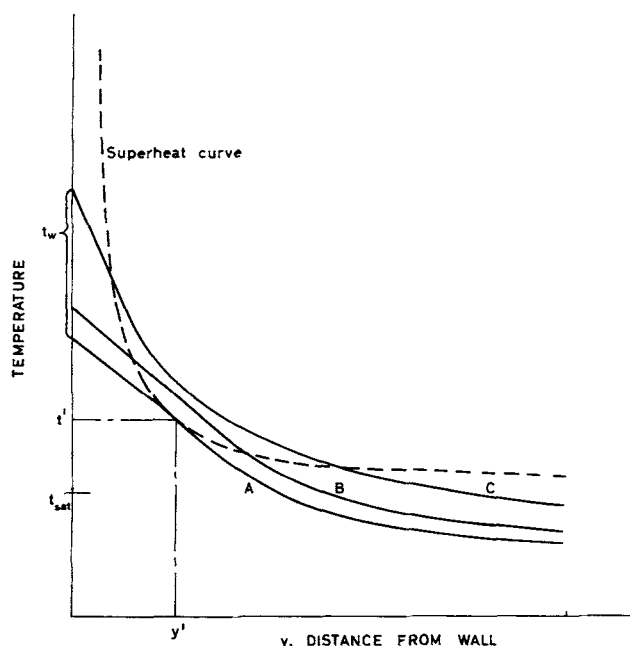


Fig. 3. An illustration of the conditions for the incipience of nucleate boiling.

Equation (15) approximates to

$$y' = \frac{2C_1 k_L S}{q_w} \quad (18)$$

and Equation (16) becomes

$$T_w - T_s = \frac{2C_1 S}{y'} + \frac{q_{wi}}{k_L} y' \quad (19)$$

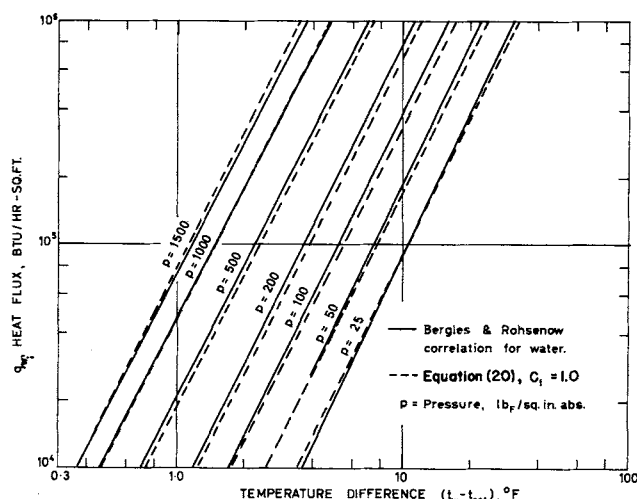


Fig. 4. A comparison of Equation (20) with the Bergles and Rohsenow correlation.

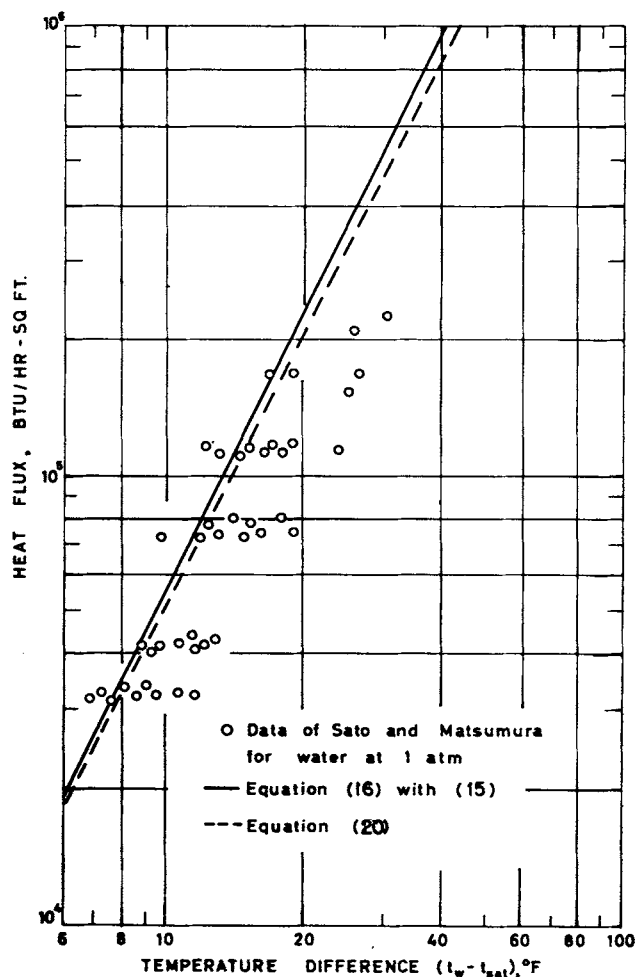


Fig. 6. A comparison of the present analysis with the data of Sato and Matsumura.

In this case it is convenient to substitute for  $y'$  from Equation (18) and to solve for the heat flux directly to give

$$q_{wi} = \frac{k_L}{8C_1 S} (T_w - T_s)^2 \quad (20)$$

Equation (20) with  $C_1 = 1$  (that is, a hemispherical bubble nucleus) is identical with the equation proposed by Sato and Matsumura [Equation (2)] though the equations are developed from rather different bubble models. Sato and Matsumura assumed a spherical bubble, but because they used the stream temperature at the mid-point of the bubble the results are identical. Figure 4 shows that the empirical correlation of Bergles and Rohsenow, Equation (1), and Equation (20) are in good agreement.

Figure 5 compares Equations (16) and (20) with Rohsenow's data (11) for water in forced convection flow boiling in a tube. The arrows marking the points of incipient boiling are Rohsenow's. In Figure 6 data of Sato and Matsumura for the onset of boiling are compared with Equations (16) and (20). The data shown, unlike Rohsenow's data in Figure 5, are all for incipient boiling conditions. It is possible that the data are inaccurate owing to the method used to measure the onset of boiling. The method was visual observation of bubble formation on the heating surface. The equations proposed here, however, appear to underpredict the incipient boiling wall superheat.

For the conditions involved in the work of the above investigators (11, 12) the incipient boiling heat fluxes

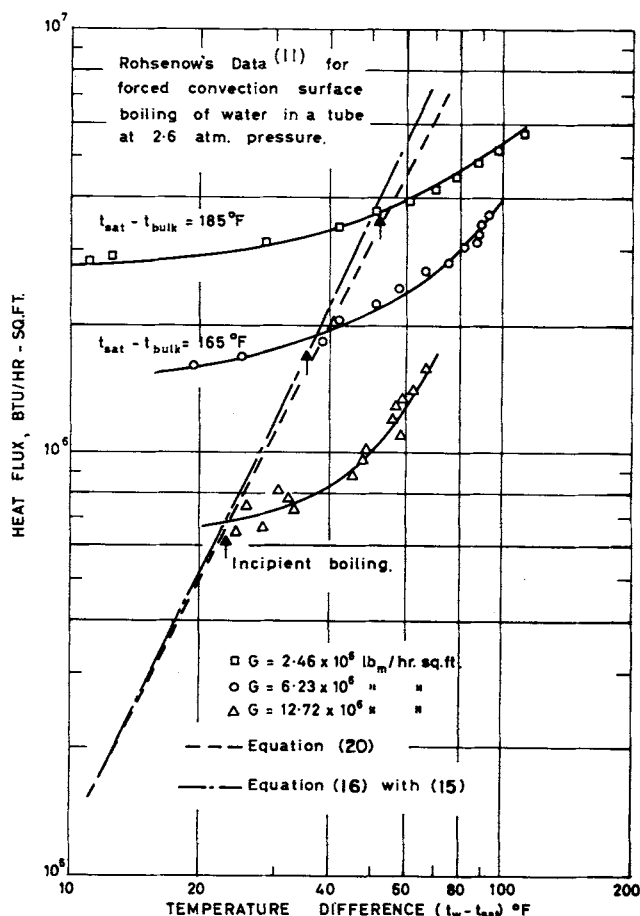


Fig. 5. A comparison of the present analysis with Rohsenow's data.

predicted by using Equations (16) and (20) are nearly the same, but for conditions involving larger wall superheats Equation (20) can be in considerable error. For many engineering applications however, Equation (20) could be used as a simple design equation.

#### APPLICATION OF THE ANALYSIS TO A SYSTEM WITH SMALL CAVITIES

Mantzouranis (16) and Backhurst (6) studied heat transfer to vapor-liquid mixtures in a forced circulation vertical tube evaporator described by Mantzouranis. They measured heat transfer coefficients, pressure gradients, and entrainment for various flow rates, pressures, and heat fluxes. They also attempted to measure and correlate the temperature differences required to initiate nucleate boiling. Mantzouranis used water in his studies, and Backhurst used benzene and toluene. In their studies the flow pattern was usually annular with dispersed annular flow occurring at high vapor flow rates, so the conditions are consistent with the assumptions involved in this analysis, and their data can be used for comparison with this analysis.

The copper tube used in their studies was initially well lapped, but not highly polished, to give a smooth surface, and it was periodically cleaned during use with Starit No. 1 to prevent any scale or excessive oxide formation. A certain amount of oxidation was inevitable in their system, and the data must be analyzed in this light. The reproducibility of the heat transfer data, which was satisfactory, is discussed elsewhere (6, 16).

Equation (16) with (15) and Equation (20) predict incipient boiling wall superheats that are considerably lower than the experimentally determined values, as shown in Figures 8 and 9. The physical properties and the experimental data for toluene are so similar to benzene that the results are nearly identical, so only the benzene data are presented.

For the conditions considered in Figures 8 and 9 Equations (15) and (18) predict  $y'$  in a range from about 3 to 20  $\mu$ , and  $r_c'$ , the critical cavity radius, is of the same order. Although these calculated critical cavity radii are small compared with typical active cavity sizes mentioned in the literature (18, 19), they are even larger than the cavity sizes computed from Rohsenow's data. Because of the substantial disagreement between the analysis (assuming a wide range of cavity sizes) and the experimental data of Backhurst and Mantzouranis, it was suspected that cavities in the size range predicted might not exist on the surface. To confirm this the authors examined specimens of the surface of the copper tube used by Backhurst and Mantzouranis to obtain information on the existing cavities.

#### EXPERIMENTAL OBSERVATIONS

Examination of the surface of the copper tube with an optical microscope indicated that partial oxidation of the surface had occurred and that no scratches, pits, or projections in the size range measurable with an optical instrument existed. Measurements of the surface roughness with a profilometer indicated that the surface was irregular and undulating. The optical microscope observations suggest that the cavity sizes involved were smaller than about 5  $\mu$ , so an electron microscope was used to examine the fine structure of the surface.

Plastic replicas of the surface were prepared by standard techniques, and a carbon film was condensed on the replica. To aid in the analysis of the topography a shadowing technique was employed which consisted of condensing gold on the carbon surface which was set at an angle to allow the gold film to be built up preferentially



Fig. 7. A typical electron micrograph of the copper heater surface.

on the side of a pit or projection. Then the plastic was dissolved and the carbon film was examined in an electron microscope.

At a magnification of 8,000 $\times$  much of the surface appeared flat, but many irregularities were observed on about 30% of the surface. Figure 7 is a typical micrograph of the surface. Surface irregularities that appear as protrusions in the micrograph correspond to pits in the original surface; for example, in Figure 7 the elliptical object directly above the scale is a projection in the surface.

Many pits and depressions in the surface in the range 0.25 to 0.75  $\mu$  were observed (the characteristic dimension here being the diameter of a circular pit, the length of the minor axis of an elliptical pit, or the width of a scratch), but no cavities with characteristic dimensions greater than approximately 2  $\mu$  were observed. Because of the irregular shapes involved and the greatly varied topography of the surface the measurements are not of high accuracy, but this does confirm that cavities of the size predicted by Equations (15) and (18) did not exist on the surface. Hence, nucleate boiling was restricted at the heat fluxes involved owing to the lack of larger cavities.

By assuming that the largest cavities observed (that is,  $r_c = 1.0\mu$ ) could be active, the experimental cavity size data can be used to compare the analysis with the heat transfer data of Backhurst and Mantzouranis. In this case nucleate boiling will occur when the superheat is sufficient to activate the largest measured cavities. Illustratively the situation corresponds to curve C in Figure 3, where the  $y$  coordinate of the point of intersection of the superheat and temperature profile curves is related to the largest cavity radius by Equation (11). Hence, calcula-

tion of  $y'$  from the measured cavity radius and substitution of this value in either Equation (16) or (19) establish equations for predicting the wall superheat required to initiate nucleate boiling as a function of the measured cavity size, the physical properties of the system, and the heat flux at the wall.

Figures 8 and 9 compare the results of this analysis with the data of Backhurst and Mantzouranis for benzene and water. For benzene and toluene Equation (19), the approximation to Equation (16), differs only slightly from the latter.

For the conditions and system studied by Mantzouranis Equation (19) is in considerable error because of the relatively high surface tension involved, so Figure 9 shows the results with Equation (16) only. Griffith and Wallis (18) reported bubble contact angles for water on a copper surface for a range of pressures including those studied by Mantzouranis. Contact angles from about 43 to 45 deg. were measured, and the calculations for Figure 9 are based on a 45-deg. contact angle. For purposes of comparison the calculations for a 90-deg. contact angle are also included on Figure 9.

Also included in Figures 8 and 9 are the predicted results from assuming a wide range of cavity sizes; considerable error is involved with this assumption. The results obtained with the measured maximum cavity size data are consistent with the experimental data.

It is to be noted that the data of Backhurst and Mantzouranis correspond to nucleate boiling suppression. In the lower part of their vertical tube nucleate boiling predominated, and in the upper part, where large vapor fractions resulted in acceleration of the liquid film, nucleate boiling was suppressed. The data used in Figures 8 and 9 do not represent a fixed position in the tube, since points for constant wall shear stress at various heat fluxes had to be extracted from their data, and this necessitated

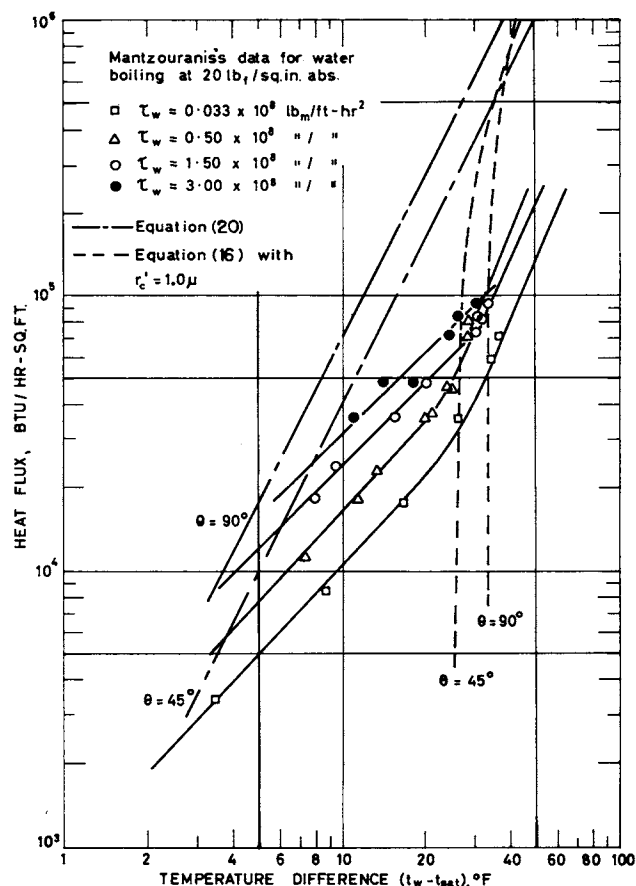


Fig. 9. A comparison of the present analysis with Mantzouranis's data.

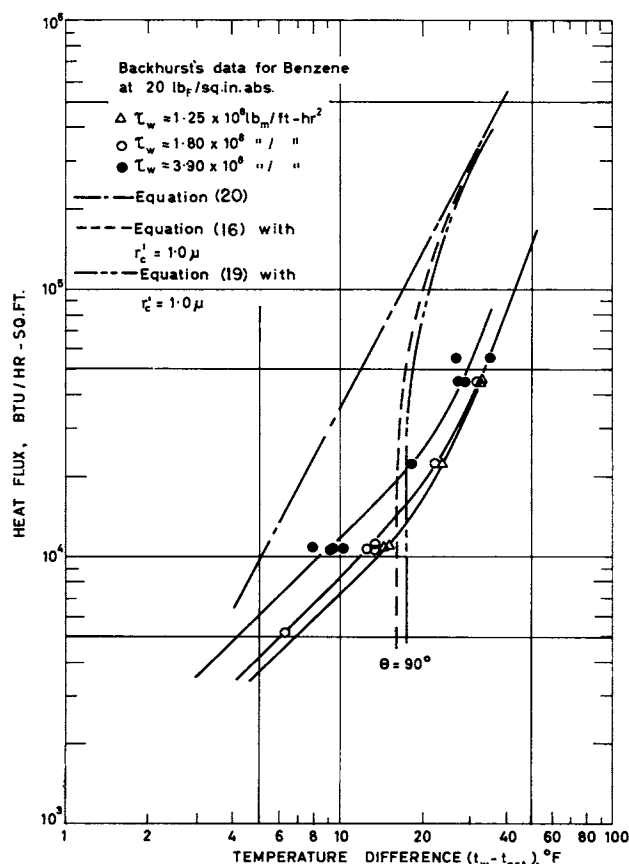


Fig. 8. A comparison of the present analysis with Backhurst's data.

the use of data taken at various points in the tube. This could explain some of the scatter in the data.

## CONCLUSIONS

1. The analysis of Bergles and Rohsenow can be treated analytically.
2. Although the criterion for the onset of nucleate boiling that was used is oversimplified, it appears satisfactory for determining an upper limit to the wall superheat required to initiate nucleate boiling.
3. The analysis need not be restricted to systems involving a wide range of cavity sizes, but if a limited cavity size range exists specific information on the maximum cavity size is needed to apply the analysis.
4. The analysis is in agreement with data on subcooled forced convection nucleate boiling of water in stainless steel and nickel tubes, and it is consistent with data on the suppression of nucleate boiling of benzene, toluene, and water in forced circulation in a vertical copper tube evaporator.
5. The size of active cavities that can be involved at the incipience of nucleate boiling under some normal engineering conditions can be of the order of  $1.0 \mu$ . Since this magnitude is below that which can be studied with optical instruments, considerable experimental difficulty is foreseen in studying cavities and bubble nuclei in such systems.

## ACKNOWLEDGMENT

The authors are indebted to A. E. B. Presland for his knowledge of the electron microscope and for his assistance; to the National Science Foundation for a postdoctoral fellowship granted to one of the authors; and to Professor K. G. Denbigh and the staff of his laboratories where the work was performed.

## NOTATION

$C_1$	= constant defined in Equation (7)
$C_2$	= constant defined in Equation (8)
$G$	= mass velocity, lb./ (hr.) (sq.ft.)
$k$	= thermal conductivity, B.t.u./ (hr.) (ft.) (°F.)
$p$	= pressure, lb./sq.ft.abs.
$q$	= heat flux, B.t.u./ (hr.) (sq.ft.)
$r$	= radius, ft.
$R$	= ideal gas constant, (ft.) (lb. <sub>f</sub> ) / (lb.) (°R.)
$S$	= group of variables defined in Equation (14)
$T$	= temperature, °R. or °F.
$\Delta T$	= temperature difference, °F.
$y$	= distance from the wall, ft.

## Greek Letters

$\theta$	= bubble contact angle
$\lambda$	= heat of vaporization, (ft.) (lb. <sub>f</sub> ) / lb.
$\rho$	= density, lb./cu.ft.
$\sigma$	= surface tension, lb. <sub>f</sub> /ft.
$\xi$	= group of variables defined in Equation (13)

## Subscripts and Superscripts

$b$	= bubble nucleus
$c$	= cavity
$'$	= coordinates of points of intersection of the superheat curve and temperature profile
$L$	= liquid phase
$s$	= property evaluated at the saturation condition
$v$	= vapor phase
$w$	= property or condition at the wall

## LITERATURE CITED

1. Leppert, G., and C. C. Pitts, in "Advances in Heat Transfer," T. F. Irvine and J. B. Hartnett, ed., Vol. 1, Academic Press, New York (1964).

2. Dengler, C. E., Ph.D. thesis, Massachusetts Inst. Technol., Cambridge (1952).
3. Davis, E. J., and M. M. David, *Can. J. Chem. Eng.*, **39**, 99 (1961).
4. Anderson, G. H., G. G. Haselden, and B. G. Mantzouranis, *Chem. Eng. Sci.*, **17**, 751 (1962).
5. Sachs, P., and R. A. K. Long, *Intern. J. Heat Mass Transfer*, **2**, 222 (1961).
6. Backhurst, J. E., Ph.D. thesis, London Univ. (1965).
7. Hsu, Y. Y., *J. Heat Transfer*, **84**, 207 (1962).
8. ———, and R. W. Graham, *Natl. Aeronaut. Space Admin. Rept. Tech. Note TN-D-594* (1961).
9. Han, C. Y., and P. Griffith, *Eng. Proj. Lab. Rept. No. 7673-19*, Massachusetts Inst. Technol. (1962).
10. Bergles, A. E., and W. M. Rohsenow, *J. Heat Transfer*, **86**, 365 (1964).
11. ———, *Dept. Mech. Eng. Tech. Rept. No. 8767-21*, Massachusetts Inst. Technol. (1962).
12. Sato, T., and H. Matsumura, *Bull. Japan Soc. Mech. Eng.*, **7**, 392 (1964).
13. Kenning, D. B. R., Oxford Univ., private communication; D. B. R. Kenning and M. G. Cooper, paper presented at Symp. Boiling Heat Transfer, Inst. Mech. Engrs., Manchester Univ. (September, 1965).
14. Gouse, S. W., and K. G. Coumou, *Eng. Proj. Lab. Rept. DSR 9649-1*, Massachusetts Inst. Technol. (1964).
15. Davis, E. J., Ph.D. thesis, Univ. Washington, Seattle (1960).
16. Mantzouranis, B. G., Ph.D. thesis, London Univ. (1958).
17. Zuber, N., comments in reference 7.
18. Griffith, P., and J. D. Wallis, *Chem. Eng. Progr. Symposium Ser.*, **56**, 49 (1960).
19. Clark, H. B., P. S. Streng, and J. W. Westwater, *Chem. Eng. Progr. Symposium Ser.*, **55**, 103 (1959).

Manuscript received July 23, 1965; revision received December 21, 1965; paper accepted February 28, 1966. Paper presented at A.I.Ch.E. Minneapolis meeting.

# Vapor-Liquid Equilibria for Five Cryogenic Mixtures

F. B. SPROW and J. M. PRAUSNITZ

University of California, Berkeley, California

Phase equilibrium data have been obtained for the binary systems nitrogen-argon and nitrogen-carbon monoxide at 83.82°K. and for the systems nitrogen-methane, argon-methane, and carbon monoxide-methane at 90.67°K. Total pressures and compositions of both phases were measured. Parameters have been calculated for the Redlich-Kister and Wilson equations for the excess Gibbs energies of the mixtures. The data are thermodynamically consistent within experimental error.

Information on the vapor-liquid equilibria of cryogenic mixtures is important both for design purposes and as a test of theories of solutions. The relatively simple molecules involved most nearly conform to the requirements of current theoretical work; however, the experimental measurements are made more difficult by the necessity of operating at low temperatures.

Equilibrium data on the systems nitrogen-argon and nitrogen-carbon monoxide have been obtained at 83.82°K.

The mixtures nitrogen-methane, argon-methane, and carbon monoxide-methane have been studied at 90.67°K. In all cases, measurements were made of the total pressure and the compositions of liquid and vapor phases ( $P$ ,  $x$ ,  $y$ ). In this way, the thermodynamic consistency of the data can be tested.

Some data for these systems are already available in the literature, although in most investigations only total pressure and liquid phase composition ( $P$ - $x$ ) data have been taken, and in this case no thermodynamic consistency test can be performed. In some previously published

F. B. Sprow is with Esso Research and Engineering Company, Baytown, Texas.